

Optimization of the surface texture for silicon carbide sliding in water

Xiaolei Wang^{a,b,*}, Koshi Adachi^a, Katsunori Otsuka^{a,c}, Koji Kato^a

^aLaboratory of Tribology, School of Mechanical Engineering, Tohoku University, Sendai 980-8579, Japan

^bCollege of Mechanical and Electrical Engineering, Nanjing University of Aeronautics and Astronautics, Nanjing 210016, China

^cKoyo Seiko Co., Ltd., 24-1 Kokubu, Higanjo-cho, Kashiwara 582-8588, Japan

Received 5 December 2005; received in revised form 28 January 2006; accepted 31 January 2006

Available online 9 March 2006

Abstract

Surface texturing has been recognized as an effective means to improve the tribological performances of sliding surfaces. Usually, generation additional hydrodynamic pressure to increase the load carrying capacity is regarded as the most significant effect of surface texture. In the case of silicon carbide sliding against identical material in water, the experimental results indicate that surface texture is also helpful to improve the running-in progress to smooth the contact surfaces, showing another reason to result in low friction. Based on the consideration of enhancing the generation of hydrodynamic pressure and improving running-in progress, a surface texture pattern, which was combined with large (circle, 350 μm in diameter) and small (rectangular, 40 μm in length) dimples, was designed to maximize the texture effect on the load carrying capacity of SiC surfaces sliding in water. The friction coefficient of such textured surface was evaluated and compared with that of untextured and those only with large or small dimples only. The friction reduction mechanisms of the patterns with different dimples in size are discussed.

© 2006 Elsevier B.V. All rights reserved.

PACS: 81.40.Pq; 46.55.td; 06.60.Vz; 47.85.Dh

Keywords: Surface texturing; SiC; Water lubrication; Running-in

1. Introduction

The surface texture, such as artificial micro-grooves or micro-dimples fabricated on the contact surfaces has proven to be effective to improve the tribological performances of sliding [1–6]. These discoveries have induced many successful applications of surface texture on golf ball, engine cylinder [7,8], sliding bearing and mechanical seal [9,10], slider and disk of hard disk driver [11,12], etc.

Many studies show that the benefits of surface texture could be obtained from boundary to hydrodynamic conditions. The friction reduction mechanisms of surface texture depend on contact conditions, materials and lubricants. Briefly, the mechanisms proposed include: decreasing contact area to reduce stiction [13]; trapping debris to prevent severe wear on the surfaces [2]; acting as reservoirs to provide lubricant to the contacting surfaces to prevent seizure [14], and generating hydrodynamic pressure to increase the load carrying capacity [15], etc.

Generally, to generate additional hydrodynamic pressure is considered as the most significant effect of surface texture under full fluid lubrication condition, so that it has attracted much more focusing historically and presently [15,16]. The main principle is that each feature acts as a hydrodynamic micro-bearing while fluid is driven and flowing over the textured surface. The pressure increased in the converging region could be greater than that of pressure decreased in diverging region of the texture since cavitations happen there. Therefore, this asymmetric hydrodynamic pressure distribution generates additional load carrying capacity for sliding surfaces. Usually, micro-grooves or micro-dimples are designed evenly distributed on the surface. The dimensions and area ratio of the texture are considered as important parameters related to the generation of hydrodynamic pressure. Recently, Etsion and co-workers have used partially textured surface to emphasize the hydrodynamic effect, showing a new attempt to optimize the surface texture design through its layout or distribution [17].

The speciality of silicon carbide (SiC) is the tribochemical reactions while it slides against identical material in water. These reactions take place during sliding with the aid of friction, remove the asperities on the surface by resolving it into

* Corresponding author. Tel.: +86 25 84893630; fax: +86 25 84234997.

E-mail address: xl_wang@nuaa.edu.cn (X. Wang).

water as silica gel [18]. After the research longer than 15 years, although scientists are still arguing on if the silica gel will contribute to the lubrication by changing the viscosity of water or not [19,20], there is no doubt that the tribochemical reactions make the establishment of full fluid lubrication easily by smoothing the contacting surfaces significantly.

Generating hydrodynamic pressure is still assumed as the main contribution of the texture in the case of SiC sliding in water. Author's previous work has demonstrated the effects of dimensions and area ratio of micro-dimples on the load carrying capacity of SiC sliding in water by experiments [21]. By the best texture pattern reported in ref. [21], which has evenly distributed dimples with diameter of $350\ \mu\text{m}$, depth around $3.2\ \mu\text{m}$ and area ratio of 4.9%, the load carrying capacity has been increased more than two times.

Besides hydrodynamic effect, the texture on the surface of SiC is also helpful for the progress of running-in process [22]. Experimental results have shown that with same running-in process, the surface with texture become smoother than that of untextured surface. This is attributed to better supply of water from dimples to satisfy the need of tribochemical reactions.

Therefore, the objective of this research is to improve the load carrying capacity of SiC sliding in water by optimizing the surface texture, obtaining the texture effects not only on hydrodynamic pressure generation, but also on running-in process promotion.

2. Experimental

2.1. Texture design

As reported in ref. [21], the pattern with the dimple diameter of $350\ \mu\text{m}$, area ratio of 4.9% and depth about $3.2\ \mu\text{m}$ showed the best results, which increased the load carrying capacity more than two times over untextured surface. The main reason was supposed to be its ability to generate hydrodynamic pressure. Since it was the pattern with sparsely distributed dimples (the pitch between dimples is 1.4 mm), it was decided to combine a pattern with densely distributed fine dimples to the pattern above to provide better water supply to the contacting area. We hope to obtain the benefits of both the hydrodynamic pressure generation and the running-in progress promotion. Fig. 1 shows three different patterns used in this experiment. Pattern (a) is the best pattern reported in ref. [21], which only has the dimples of $350\ \mu\text{m}$ in diameter. Pattern (b)

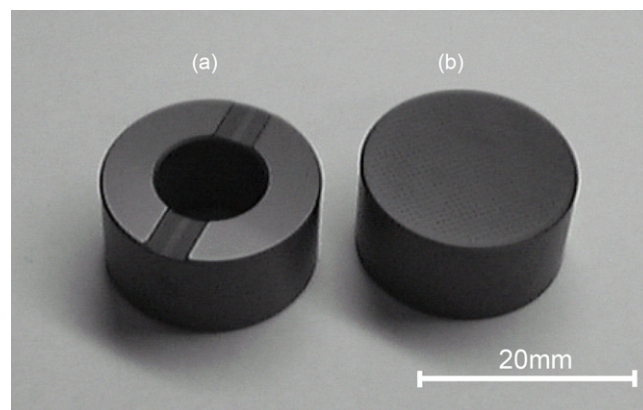


Fig. 2. Specimens: (a) ring (upper specimen) and (b) disk (lower specimen).

only has the small square dimples with the side length of $40\ \mu\text{m}$. Pattern (c) is the pattern combined with (a) and (b). Because pattern (b) has a large number of small dimples, using the shape of square instead of circle could significantly save the computing time for the generation of photo mask used for lithography process.

2.2. Specimens

The friction tests were carried out between the flat surfaces of a ring [Fig. 2(a), upper specimen] and a disk [Fig. 2(b), lower specimen]. Both the ring and disk were made of SiC sintered after CIP process. The mechanical properties of the material are listed in Table 1. The centre hole of the ring was used for water supply. Two grooves were made on the flat surface of the ring to guide water from the centre hole to the contact surfaces. The contact area of the ring and disk during test is about $1.9\ \text{cm}^2$.

Both the flat surfaces of upper and lower specimens were ground and polished to a roughness Ra of around $0.02\ \mu\text{m}$. And then, the dimple patterns shown in Fig. 1 were fabricated on the flat surface of the disk by lithography and reactive ion etching (RIE).

The detail process of texture fabrication shown in Fig. 3 contains the following steps:

- The surface of SiC disk was cleaned with standard cleaning procedure.
- A Cr film of approximately $1\ \mu\text{m}$ was coated on the cleaned SiC surface by sputtering as a protection film during RIE.

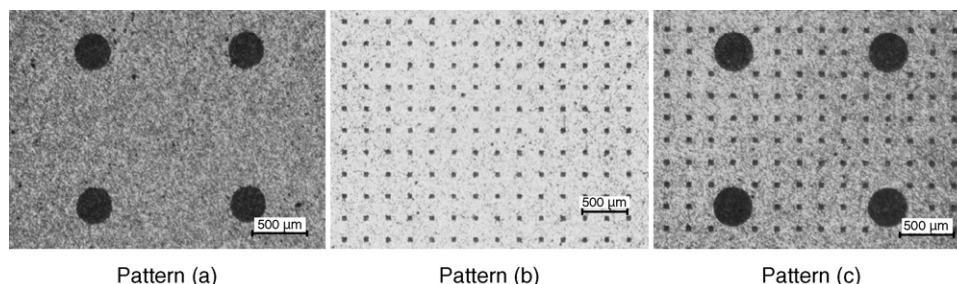


Fig. 1. Three patterns of surface texture used in this experiment: (a) large dimples only; (b) small dimples only; and (c) large dimples mixed with small dimples.

Table 1
Mechanical properties of silicon carbide

Density (kg/m ³)	3100
Pore ratio (%)	0.1
Young's modulus (GPa)	390
Poisson's ratio	0.16
Bending strength (MPa)	490
Rockwell hardness	94
Coefficient of linear thermal expansion (K ⁻¹)	4.5×10^{-6}
Thermal conductivity (W/(m K))	158
Fracture toughness (MPa m ^{1/2})	3.5–4.5

- (c) A high-resolution negative photoresist layer was coated on the Cr layer by a spin-coater.
 (d) The photoresist layer was patterned with standard lithograph process.
 (e) The pattern was transferred to Cr film by wet etching.
 (f) Photoresist layer was removed using solvent.
 (g) The pattern was transferred to SiC by RIE. The reaction was: $\text{SiC} + \text{SF}_6 \rightarrow \text{SiF}_4 + \text{CF}_n + \dots$
 (h) Cr film was removed by wet etching.

The detail dimensions and area ratios of the patterns fabricated are listed in Table 2.

2.3. Tester

Fig. 4 shows the schematic diagram of the tester used in this experiment.

The ring is mated to the disk and driven by a motor. The disk is fixed in a holder supported by a half-spherical tip so that the flat surface of the disk is self-aligned to the surface of the ring. Load is applied by a hydraulic system from the bottom of the disk. Purified water was filled into the center hole of the ring with a supply rate of 60 ml/min. The temperature of the water supplied to the friction surfaces was controlled at around 18 °C. Load and friction torque were detected by load cells. An air bearing is used to support the disk so that the accuracy of friction torque measurement could reach the level of 0.001 N m.

A protecting system will be activated to stop the load applying system and the driving motor when friction force reaches the threshold value, which was predefined to 40 N in this test.

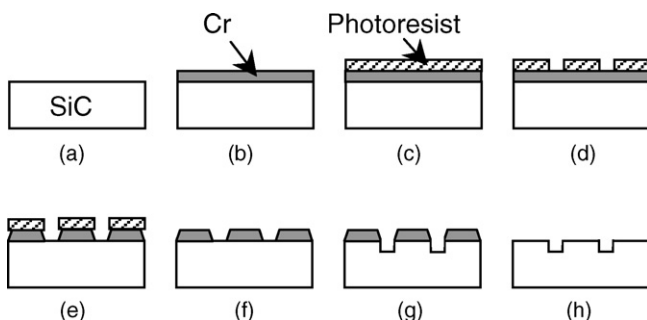


Fig. 3. Fabrication process of surface texture.

Table 2
Dimensions and area ratios of the patterns used

Texture pattern	(a) Large only	(b) Small only	(c) Mixed
Diameter/side length (μm)	350	40	40, 350
Depth (μm)	2.7–7.9	2.6–7.0	3.4–8.0
Pitch (μm)	1400	200	200, 1400
Area ratio (%)	4.9	4.0	8.5

2.4. Multi-step loading running-in process

It is known that a running-in process is critical for a new SiC surface to obtain a friction in steady state while it slides in water against identical material. The wear mode of SiC surfaces depends on load, sliding speed, lubrication and contact condition of asperities. If the tribochemical wear is controlled as the dominant wear mode, SiC has an ideal running-in process, while the surface is becoming smooth resulting in the rapid decrease in friction. A rapid increase of the load will easily induce mechanical wear, which will damage the brittle surface of SiC. Therefore, a multi-step loading running-in process was carried out for all specimens before friction test. As shown in Fig. 5, every specimen was run-in at a rotational speed of 800 rpm with water lubrication. The load increment of each step was 98 N. The load was increased when friction became stable, or the previous running-in step was as long as 1 h. The increase of the load was repeated as many times as possible until the friction no longer decreased or rapidly increased to activate the protecting system to stop the tester. The understanding of this moment is, either there is no improvement to the contact condition; or mechanical wear is starting. The peak value of friction force shown in Fig. 5 might not be presented correctly since it happened at a moment of load increasing so that the record system might not be fast enough to catch the peak value.

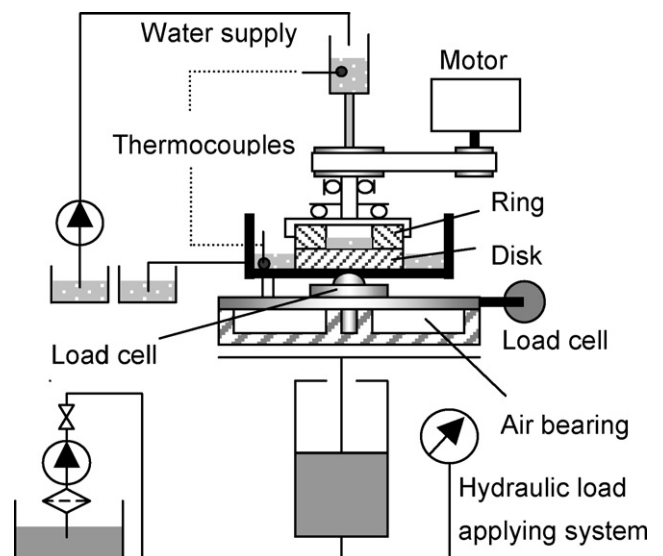


Fig. 4. Schematic diagram of the tester.

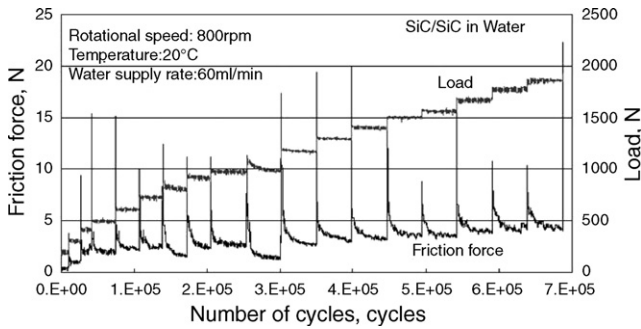


Fig. 5. The multi-step loading running-in process at the rotational speed of 800 rpm.

2.5. Results

After the multi-step loading running-in process, friction was measured at 800 rpm with a load, which was continually increased from zero. Fig. 6 shows the friction coefficients of the specimens, untextured and textured with pattern (a), (b) and (c), respectively. Some extremely low friction data was not presented in this figure. The reason is that all textured specimens had the friction coefficient lower than 0.001 while load was low, so that a zero drift error of sampling system may cause the friction recorded as negative. This problem happened for the pattern (a) at loads below 2500 N and pattern (b) at loads below 1800 N. Some high friction data of pattern (a) was also lost. This was because the friction increased so rapidly while the load was higher than 3200 N that the recorder was not fast enough to catch the data.

All the specimens had a load range with relative low and stable friction coefficient. After the load exceeded this range, the friction increased rapidly. The range with low and stable friction can be considered as hydrodynamic lubrication condition since the friction coefficients were extremely low and less responsive to the increase of load. For the friction coefficient in this range, it is obvious that textured surfaces reduced the friction. But it is hard to compare the friction coefficients between the textured surfaces because their values were lower than 0.001, which is around the level of zero drift of sampling system.

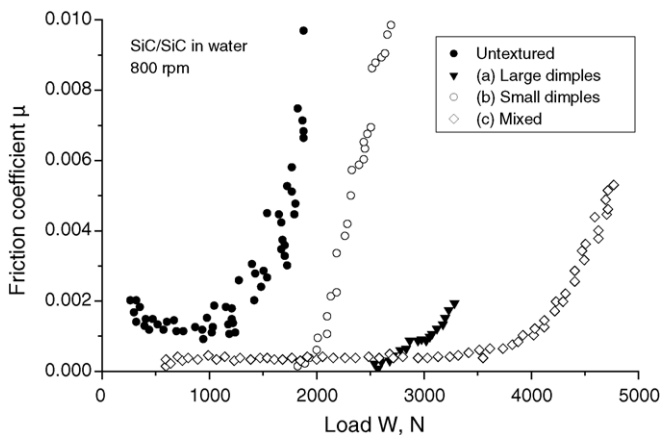


Fig. 6. Friction coefficient vs. load of untextured and textured specimens at 800 rpm.

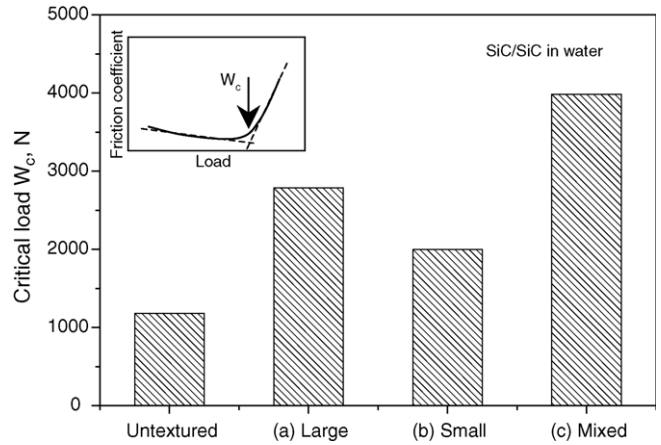


Fig. 7. The critical load of untextured and textured specimens.

The value of the load at which friction begins to increase (W_c , as shown in Fig. 7) is the transition load of lubrication mode between full fluid lubrication and mixed lubrication. This load was defined as the critical load in this research to evaluate the texture effect. Higher critical load means greater load carrying capacity since the lubrication film could be established in a wider load range. Fig. 7 shows the definition and the values of the critical load of each untextured and textured specimens. It is found that critical load of all the textured specimens were greater than that of untextured specimen. Although pattern (a) and (b) have similar or same depth and area ratio, agree with the results reported in ref. [21], the critical load of pattern (a) was almost 40% higher than that of pattern (b). The pattern combined with the small and large dimples had the greatest value of critical load in this research, which was 3.3 times as much as that of untextured surface.

2.6. Discussions

The pattern with large dimples was the best pattern which represent the greatest critical load reported in ref. [21]. Based on the simulation with Reynolds equation, generation of hydrodynamic pressure was assumed to be the main contribution of pattern (a) due to its proper depth-to-diameter ratio (h/d) and the

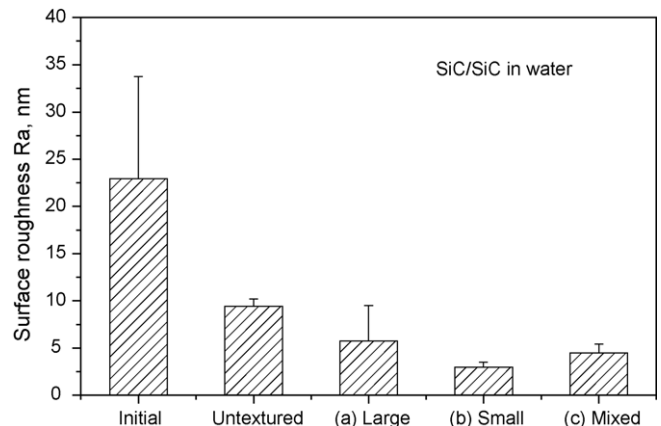


Fig. 8. Surface roughness of initial surface and after running-in process.

area ratio of dimple pattern. Relatively, the depth-to-diameter ratio of the pattern with small dimples is much higher than that of pattern (a). Therefore, the critical load of the pattern with small dimples is not as high as that of the pattern with large dimples.

Fig. 8 shows the surface roughness before and after running-in process. From the initial roughness R_a around 22 nm, the running-in process smoothed all the surfaces to R_a below 10 nm. It is obvious that surface texture was helpful for the progress of running-in since all the textured surfaces were smoother than that of untextured. It was thought that although the area ratio of the pattern with small dimples is not higher than the pattern with large dimples, the densely distributed fine dimples might provide a better water supply to the contacting area for the tribochemical reaction, therefore, it resulted in the lowest surface roughness. This effect could be also found when this pattern was added to the pattern with large dimples only. The roughness of the surface mixed with small and large dimples is lower than that with large dimples only, although it was not as smooth as that with small dimples only.

Critical load is the load where lubrication condition transits between full fluid and mixed lubrication. For the establishment of full fluid lubrication, the theoretical film thickness depends on hydrodynamic pressure between surfaces, and the existence of real fluid film depends on the comparison of theoretical film thickness and surface roughness. Therefore, the pattern that had the combination of large and small dimples exhibited the beneficial effects obtained by the individual patterns, i.e., hydrodynamic pressure generated by surface texture like that of the pattern (a) and smooth surface due to the running-in process with densely distributed fine dimples like pattern (b). Therefore, the specimen with mixed dimples exhibited the greatest critical load in this experiment.

3. Conclusions

With the hypothesis that surface texture is capable of generating hydrodynamic pressure and improving the running-in progress of silicon carbide sliding in water, a textured pattern combined with large dimples and small dimples was designed to improve the load carrying capacity of SiC sliding in water. The texture effects were evaluated on the aspects of friction coefficient and the critical load W_c for the transition of lubrication mode from full fluid to mixed. By comparing the untextured with textured, it was found that the pattern mixed with the large dimples (350 μm) and small dimples (40 μm) resulted in higher critical load over that with small or large dimples only, and three times greater than that of untextured specimen. This investigation reveals great potential on the improvement of the load carrying capacity by the texture designing based on comprehensive understanding of the friction reduction mechanisms of surface texture.

References

- [1] R. Ranjan, D.N. Lambeth, M. Tromel, P. Goglia, Y. Li, Laser texturing for low-flying-height media, *J. Appl. Phys.* 69 (8) (1991) 5745–5747.
- [2] N.P. Suh, M. Mosleh, P.S. Howard, Control of friction, *Wear* 175 (1–2) (1994) 151–158.
- [3] M. Geiger, S. Roth, W. Becker, Influence of laser-produced microstructures on the tribological behaviour of ceramics, *Surf. Coat. Technol.* 100–101 (1998) 17–22.
- [4] G. Dumitru, V. Romano, H.P. Weber, H. Haefke, Y. Gerbig, E. Pfluger, Laser microstructuring of steel surfaces for tribological applications, *Appl. Phys. A Mat. Sci. Process.* 70 (4) (2000) 485–487.
- [5] M. Wakuda, Y. Yamauchi, S. Kanzaki, Y. Yasuda, Effect of surface texturing on friction reduction between ceramic and steel materials under lubricated sliding contact, *Wear* 254 (2003) 356–363.
- [6] X. Wang, K. Kato, K. Adachi, K. Aizawa, The effect of laser texturing of SiC surface on the critical load for the transition of water lubrication mode from hydrodynamic to mixed, *Tribol. Int.* 34 (2001) 703–711.
- [7] E. Willis, Surface finish in relation to cylinder liners, *Wear* 109 (1–4) (1986) 351–366.
- [8] H. Ogihara, T. Kido, H. Yamada, M. Murata, S. Kobayashi, Technology for reducing engine rubbing resistance by means of surface improvement, *HONDA R&D Tech. Rev.* 12 (2) (2000) 93–98.
- [9] X. Wang, K. Kato, Improving the anti-seizure ability of SiC seal in water with RIE texturing, *Tribol. Lett.* 14 (4) (2003) 275–280.
- [10] I. Etsion, G. Halperin, V. Brizmer, Y. Kligerman, Experimental investigation of laser surface textured parallel thrust bearings, *Tribol. Lett.* 17 (2) (2004) 295–300.
- [11] A. Khurshudov, B. Knigge, F.E. Talke, P. Baumgart, A. Tam, Tribology of laser-textured and mechanically-textured media, *IEEE Trans. Magn.* 33 (5) (1997) 3190–3192.
- [12] L. Zhou, K. Kato, N. Umehara, Y. Miyake, Nanometre scale island-type texture with controllable height and area ratio formed by ion-beam etching on hard-disk head sliders, *Nanotechnology* 10 (4) (1999) 363–372.
- [13] P. Baumgart, D.J. Krajnovich, T.A. Nguyen, A.C. Tam, A new laser texturing technique for high-performance magnetic disk drives, *IEEE Trans. Magn.* 31 (6) (1995) 2946–2951.
- [14] U. Pettersson, S. Jacobson, Influence of surface texture on boundary lubricated sliding contacts, *Tribol. Int.* 36 (2003) 857–864.
- [15] D.B. Hamilton, J.A. Walowitz, C.M. Allen, A theory of lubrication by micro-irregularities, *J. Basic Eng.* (1966) 177–185.
- [16] I. Etsion, L. Burstein, A model for mechanical seals with regular microsurface structure, *Tribol. Trans.* 39 (3) (1996) 677–683.
- [17] V. Brizmer, Y. Kligerman, I. Etsion, A laser surface textured parallel thrust bearing, *Tribol. Trans.* 46 (3) (2003) 397–403.
- [18] S. Sasaki, The effects of water on friction and wear of ceramics, *J. Jpn. Soc. Lubr. Eng.* 33 (8) (1988) 620–628.
- [19] L. Jordi, C. Iliev, T.E. Fischer, Lubrication of silicon nitride and silicon carbide by water: running in, wear and operation of sliding bearings, *Tribol. Trans.* 17 (3) (2004) 367–376.
- [20] X. Wang, K. Kato, K. Adachi, The critical condition for the transition from HL to ML in water-lubricated SiC, *Tribol. Lett.* 16 (4) (2004) 253–258.
- [21] X. Wang, K. Kato, K. Adachi, K. Aizawa, Loads carrying capacity map for the surface texture design of SiC thrust bearing sliding in water, *Tribol. Int.* 36 (2003) 189–197.
- [22] X. Wang, K. Kato, K. Adachi, Running-in effect on the load-carrying capacity of a water-lubricated SiC thrust bearing, *J. Eng. Tribol.* 219 (2) (2005) 117–124.